JOURNAL OF MATERIALS SCIENCE 31 (1996) 3559–3565

Carbothermal reduction and nitridation of aluminium hydroxide

WEN-HONG TSENG, CHUN-I LIN
Department of Chemical Engineering, National Taiwan Institute of Technology, Taipei, Taiwan 106

Carbothermal reduction and nitridation of aluminium hydroxide was investigated by weight-loss measurement and X-ray diffraction. Experimental results indicated that aluminium hydroxide was first dehydrated to aluminium oxide and then reduced and nitrided to aluminium nitride. Aluminium oxynitride and Al_2O were found to be intermediate products. The reaction rate was found to be increased by increasing the nitrogen flow rate, the molar ratio of $C/Al(OH)_3$, or reaction temperature. The rate was also found to be increased by decreasing the sample size, the grain sizes of carbon or aluminium hydroxide or initial bulk density. Empirical rate expressions of the conversion of $Al(OH)_3$ and carbon, as well as the yield of AlN, were also determined.

1. Introduction

α-Al_2O_3 is conventionally used as a precursor to synthesize aluminium nitride by the method of carbothermal reduction and nitridation [1–6]. The reaction is known to be enhanced, reaction temperature and time are reduced, the oxygen content of AlN is reduced and the quality of the AlN product is improved; that is, if α-Al_2O_3 is replaced by $Al(OH)_3$ [5, 7]. Unfortunately, the carbothermal reduction and nitridation of aluminium hydroxide have received limited attention [6–12]. Literature involving the kinetics of this reaction is especially rare [7]. Cho and Charles [7] observed that the overall reaction rate increased with decreasing $Al(OH)_3$ particle size and increasing nitrogen flow rate. They also found that the particle morphologies of the $Al(OH)_3$ powders did not change during the reaction. Ish-Shalom pointed out that aluminium oxynitride was the intermediate product during reaction [8]. Mimoto and Yoshioka [10] reported that no appreciable evaporation of aluminium species occurred during the preparation of AlN. Inoue *et al.* [5] stated that the skeleton of raw powder remained in the synthesized AlN powder shape.

The overall chemical reaction of this system can be written as

$$2Al(OH)_3 + 3C + N_2 \rightarrow 2AlN + 3CO + 3H_2O \quad (1)$$

The intermediate products and the kinetics of this reaction, have been examined in this work. The effects of the following factors on the rates of reaction were investigated: gas flow rate, sample height, reaction temperature, molar ratio of $C/Al(OH)_3$, grain size and initial bulk density.

2. Experimental procedure

Sample preparation, the apparatus and procedure are similar to those described elsewhere [6] except that Al_2O_3 was replaced by $Al(OH)_3$.

Nitrogen used in this study was produced by Lien-Hwa Industrial Gases Co. Ltd with a minimum purity of 99.995%. Fine powder pure aluminium hydroxide was supplied by E. Merk Darmstadt and acetylene carbon black by Stream Chemicals, Inc. Powders of $Al(OH)_3$ and carbon black were separately dried and screened. These powders with known grain sizes and predetermined proportions were mixed in a ball mill for 43 200 s with ethanol as a dispersing medium. Next, the mixed samples were dried in a nitrogen stream at 373 K until no further weight loss, and then transferred to an alumina crucible of 0.024 m diameter and 0.002 m height. The weights of solid samples were in the range of 8.47×10^{-4} to 6.77×10^{-3} kg.

Reactions were carried out in a horizontal alumina tube heated by a furnace. The reaction tube was heated at room temperature and the nitrogen was introduced to the tube during the heating up period. When the temperature reached the desired one and had been stably maintained for about 200 s, the solid sample was pushed by an alumina rod from the cold end of the tube to the reaction zone for reaction. The pressure in the reaction tube was maintained at 0.01–0.03 m H_2O higher than atmospheric. After a predetermined time, the solid sample was removed and quenched in an argon stream.

After measuring the weight, the solid sample was calcined at 973 K for 10 800 s. The weight of the calcined sample was redetermined. The amount of residual carbon in the solid sample was calculated from the weights before and after calcination. Finally, the

0022–2461

aluminium nitride content in the sample was determined from X-ray diffractometery.

Thermogravimetric analysis/differential thermal analysis was performed on aluminium hydroxide. Surface areas of several aluminium compounds were determined using a Micrometritics ASAP 2000 surface area meter.

3. Results and discussion

3.1. Chemical reactions

3.1.1. Dehydration of aluminium hydroxide

Aluminium hydroxide is dehydrated to several phases of aluminium oxide at higher temperatures. TGA/DTA results (Fig. 1) indicated that the solid sample started to lose weight from about 503 K; in addition, the weight of the sample would become stable at about 900 s. The temperature of the dehydration process was low and the rate was high. All aluminium hydroxide in the solid sample is converted to aluminium oxide during the initial stage of reduction and nitridation. Therefore, the reactant involved in the reaction is Al_2O_3 not $Al(OH)_3$ and the reactions can be written as

$$2Al(OH)_3 \rightarrow Al_2O_3 + 3H_2O \quad \text{(very fast)} \quad (2)$$

$$Al_2O_3 + \frac{(m+2)}{3} C + \frac{(m+2)}{3} N_2 \rightarrow 2\frac{(m+2)}{3} AlN + mCO + CO_2 \quad (3)$$

Fig. 2 shows the X-ray diffraction pattern of $Al(OH)_3$ before and after calcining at 973 K for 1800 s under a helium atmosphere. This figure indicates that a large quantity of $Al(OH)_3$ has been converted to γ-Al_2O_3 after calcination.

The surface areas of several aluminium compounds are listed in Table I. This table reveals that the surface area of uncalcined $Al(OH)_3$ is 6.26×10^3 $m^2 kg^{-1}$ and that of calcined $Al(OH)_3$ has been increased to 1.49×10^5 $m^2 kg^{-1}$ which is even higher than that of γ-Al_2O_3, 1.02×10^5 $m^2 kg^{-1}$. The surface area of α-Al_2O_3 is only 7.02×10^3 $m^2 kg^{-1}$. The reaction rate is normally proportional to the surface area of solid reactant. Therefore, the order of the rate of reduction and nitridation is $Al(OH)_3 > \gamma$-$Al_2O_3 > \alpha$-Al_2O_3. Experimental results in Fig. 3 verify this expectation; the results coincide with previously published data [5, 7], and indicate that unstable and high reactivity phases of Al_2O_3, e.g. γ, δ, θ, κ, λ and χ, are formed after calcination, as reported by Candela and Perlmutter [13] and Sato [14].

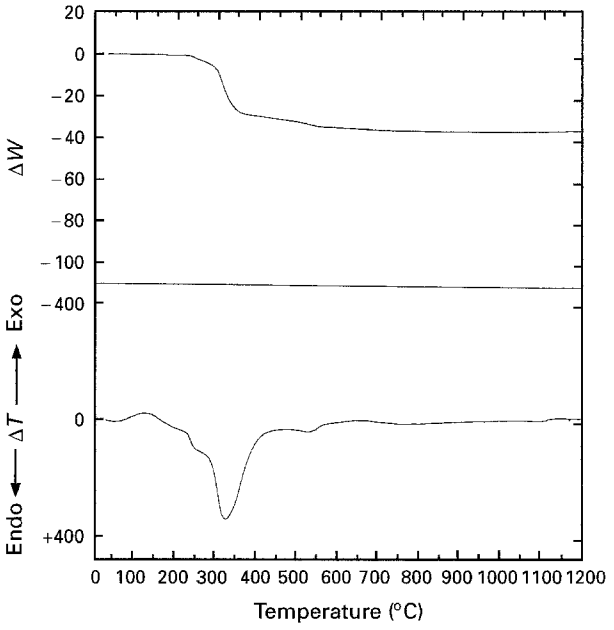

Figure 1 TGA/DTA curves for $Al(OH)_3$.

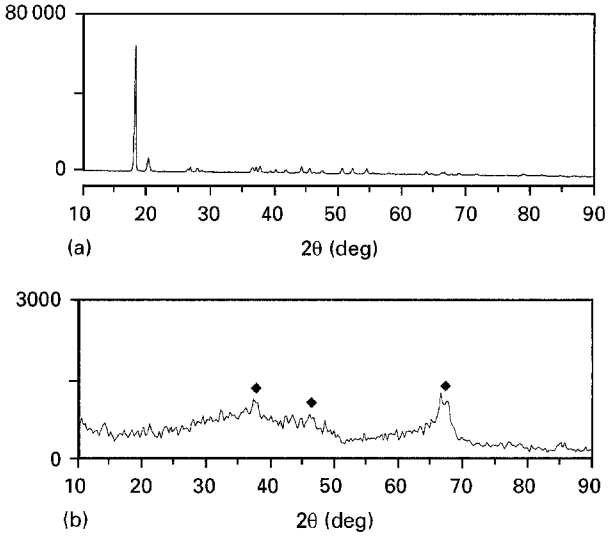

Figure 2 X-ray diffraction patterns of (a) $Al(OH)_3$, and (b) $Al(OH)_3$ calcined at 973 K for 1800 s. (◆) γ-Al_2O_3.

TABLE I Surface areas of aluminium compound

Aluminium compound	Surface area ($m^2 kg^{-1}$)
$Al(OH)_3$	6.26×10^3
$Al(OH)_3$ heated at 973 K for 1800 s	1.49×10^5
α-Al_2O_3	7.02×10^3
γ-Al_2O_3	1.02×10^5

3.1.2. Other intermediate products

The X-ray diffraction pattern of the solid sample after reduction and nitridation, indicates the presence of Al_2O_3, AlON and AlN. The amount of aluminium oxynitride AlON contained in the sample cannot be directly determined from the X-ray diffraction pattern because it is unstable and cannot be purchased to prepare the calibration curve. However, the amount of AlON can be qualitatively determined through the comparison of the intensities at $2\theta = 45.2°$. The higher the intensity would imply the larger the amount of AlON. A plot of the intensity of the AlON peak against reaction time at different reaction temperatures is depicted in Fig. 4, which reveals that when the reaction time is increased, the amount of AlON is increased, reaches a maximum, decreases and then disappears. As the reaction temperature is increased, the peak is higher and appears in a shorter time.

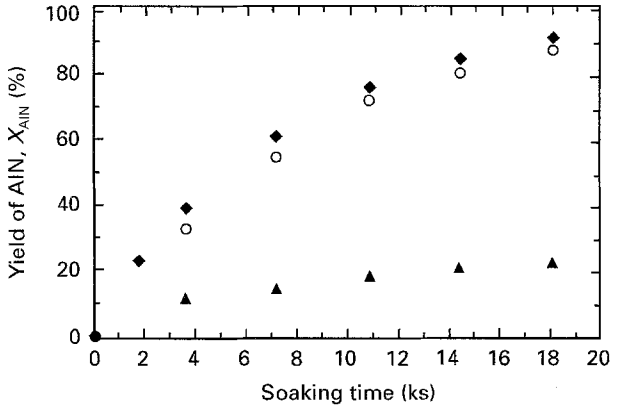

Figure 3 Plot of the yield of AlN against soaking time, showing the effect of various aluminium compounds. Gas flow rate = 2.083×10^{-5} m^3 s^{-1}, sample height = 0.002 m, temperature = 1723 K, C/Al(OH)$_3$ molar ratio = 3/1, carbon and Al(OH)$_3$ grain size = 0.042 mm, initial bulk density 510 kg m^{-3}. (◆) Al(OH)$_3$, (○) γ-Al_2O_3, (▲) α-Al_2O_3.

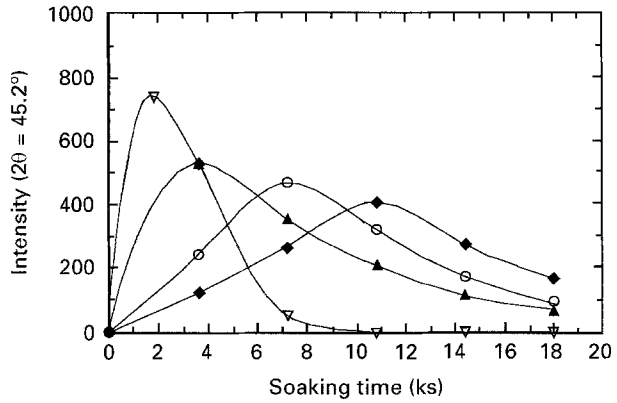

Figure 4 Plot of the intensity of AlON against soaking time, at (◆) 1573 K, (○) 1623 K, (▲) 1673 K, (▽) 1723 K.

If the intensities of Al_2O_3, AlON and AlN are plotted against reaction time, the curves are as shown in Fig. 5. As reaction time increased, the amount of Al_2O_3 decreases monotonically; the amount of AlON increases, reaches a peak and then decreases; the amount of AlN increases monotonically. This is easily found to be a system of series reactions in which Al_2O_3 is a reactant, AlON is an intermediate product, and AlN is a product.

The above findings agree with those of Ish-Shalom [8].

The other intermediate product was Al_2O gas. A detailed discussion of this is presented below.

3.2. Reaction kinetics

Six series of experiments were performed to examine the kinetics of this reaction. In each of the series, one of the following variables was varied: i.e. gas flow rate, sample height, reaction temperature, molar ratio of C/Al(OH)$_3$, grain size and initial bulk density. The values of the variables studied are listed in Table II. The italicized values are the standard operating variables. That is, when the effect of that variable is not

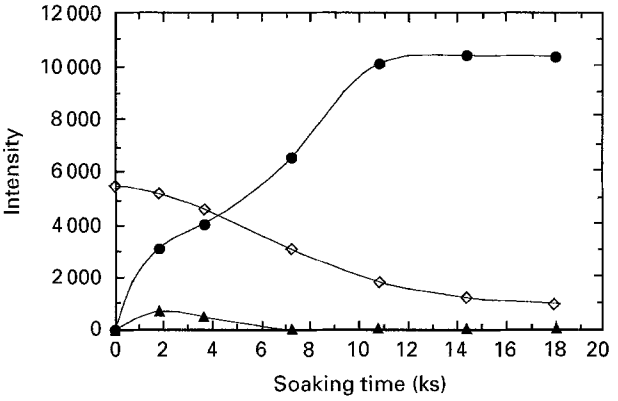

Figure 5 Plots of the intensities of (◇) Al_2O_3, (▲) AlON and (●) AlN against soaking time. 2θ: (◇) 43.3°, (▲) 45.2°, (●) 33.2°.

TABLE II Values of the operating variables

Operating variable	value
Gas flow rate (m^3 s^{-1})	4.167×10^{-6}, 9.167×10^{-6}, 1.333×10^{-5}, 1.833×10^{-5}, $\underline{2.083 \times 10^{-5}}$, 2.250×10^{-5}, 2.750×10^{-5}
Sample height (m)	0.001, $\underline{0.002}$, 0.004, 0.006, 0.008
Reaction temperature (K)	1573, 1623, 1673, $\underline{1723}$, 1773
C/Al(OH)$_3$ molar ratio	1.5/1, $\underline{3/1}$, 6/1
Carbon grain size (mm)	$\underline{0.042}$, 0.0675, 0.1155
Al(OH)$_3$ grain size (mm)	$\underline{0.042}$, 0.0675, 0.1155
Initial bulk density (kg m^{-3})	270, 370, $\underline{510}$

studied, its value is held at the italicized value in that series of experiments. Those experimental results are presented by plotting the conversion of Al(OH)$_3$ and C, $X_{Al(OH)_3}$ and X_C, respectively, as well as the yield of AlN, X_{AlN}, versus time, and the conversions and the yield are defined as follows

$$X_{AlN} = \frac{C_{AlN}}{C^0_{Al(OH)_3}} \quad (4)$$

$$X_{Al(OH)_3} = \frac{\Delta C_{Al(OH)_3}}{C^0_{Al(OH)_3}} \quad (5)$$

$$X_C = \frac{\Delta C_c}{C^0_C} \quad (6)$$

where C_{AlN} is the number of moles of AlN at time t, $C^0_{Al(OH)_3}$ the initial moles of Al(OH)$_3$, C^0_C the initial moles of carbon, $\Delta C_{Al(OH)_3}$ the consumed moles of Al(OH)$_3$ at time t, and ΔC_C the consumed moles of carbon at time t.

3.2.1. Effect of gas flow rate

The effects of gas flow rate on the yield of AlN and conversions of Al(OH)$_3$ and carbon are shown in Figs 6–8, respectively. The figures indicate that the faster the gas flow, the faster is the reaction. When the nitrogen flow rate exceeds 2.083×10^{-5} m^3 s^{-1}, the reaction rate is no longer accelerated, which means that when the temperature is 1723 K and the sample size is 0.002 m, mass transfer resistance in the gas film

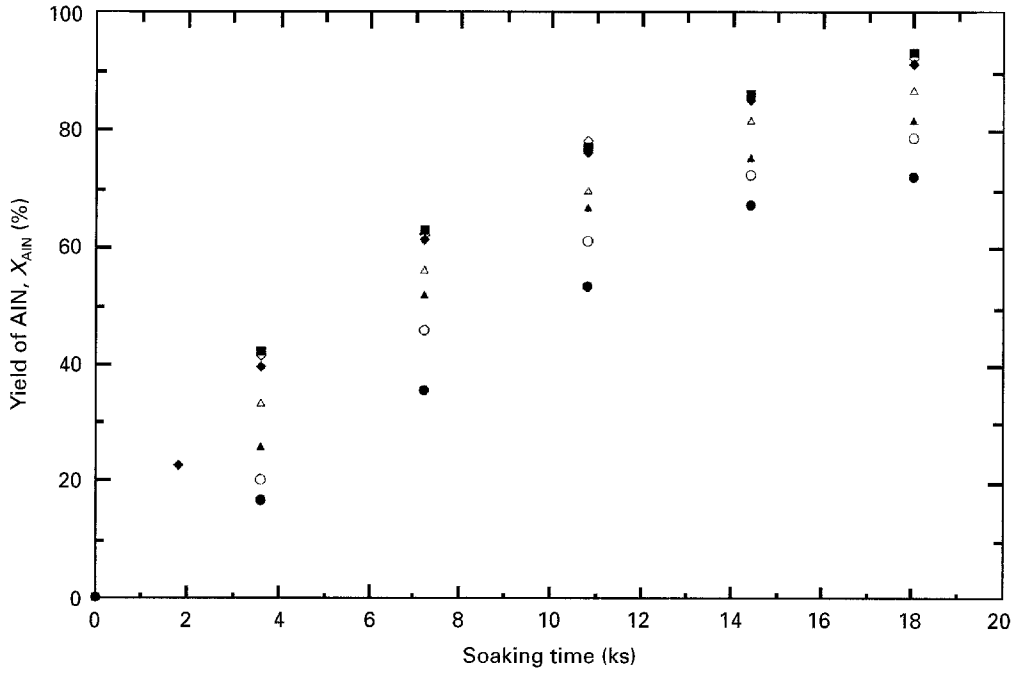

Figure 6 Plot of the yield of AlN against soaking time, showing the effect of gas flow rate ($m^3 s^{-1}$): (●) 4.167×10^{-6}, (○) 9.167×10^{-6}, (▲) 1.333×10^{-5}, (△) 1.833×10^{-5}, (◆) 2.083×10^{-5}, (◇) 2.250×10^{-5}, (■) 2.750×10^{-5}.

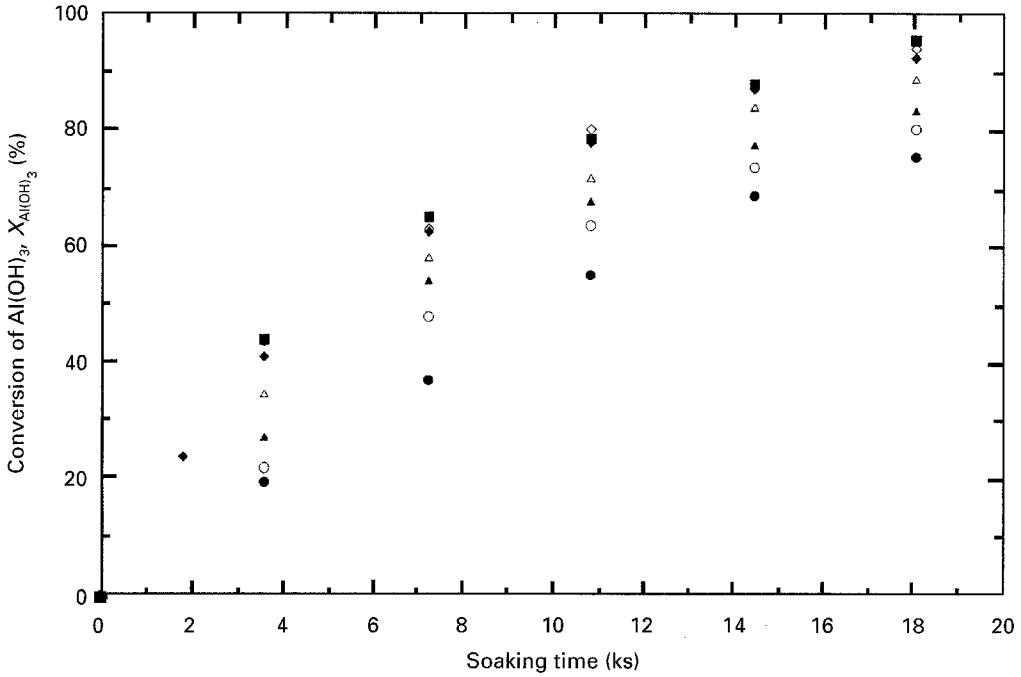

Figure 7 Plot of the conversion of $Al(OH)_3$ against soaking time, showing the effect of gas flow rate. For key, see Fig. 6.

can be neglected. Thereafter, the nitrogen flow rate was maintained at 2.083×10^{-5} $m^3 s^{-1}$ in all experimental runs.

A comparison of Figs 6 and 7 reveals that the fraction of $Al(OH)_3$ converted was, under all conditions, higher than that of the yield of AlN.

Chen *et al.* [6] proposed the following reasoning to account for this phenomenon. An intermediate gas product, Al_2O, is formed before Al_2O_3 is converted to AlN. Most of the Al_2O finally converts to AlN. However, a small amount of Al_2O diffuses from the solid matrix to the sample surface and is carried away by the nitrogen stream. This supports the presentation of an intermediate product of Al_2O, as mentioned above.

3.2.2. Effect of sample height

The effect of sample height on the yield of AlN is shown in Fig. 9. This figure indicates that the smaller the sample size, the higher will be the yield of AlN. When the sample height is less than 0.002 m, the reaction rate is no longer enhanced, thereby suggesting that the so-called "reaction controlled region" has been reached. Data obtained in this region are

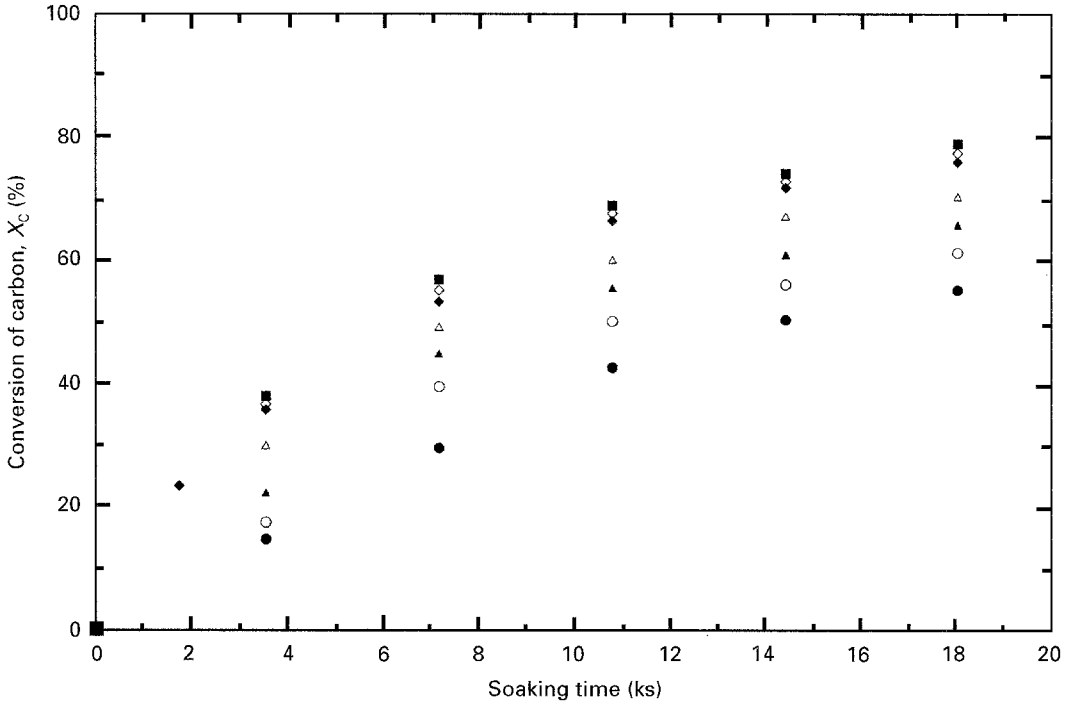

Figure 8 Plot of the conversion of carbon against soaking time, showing the effect of gas flow rate. For key, see Fig. 6.

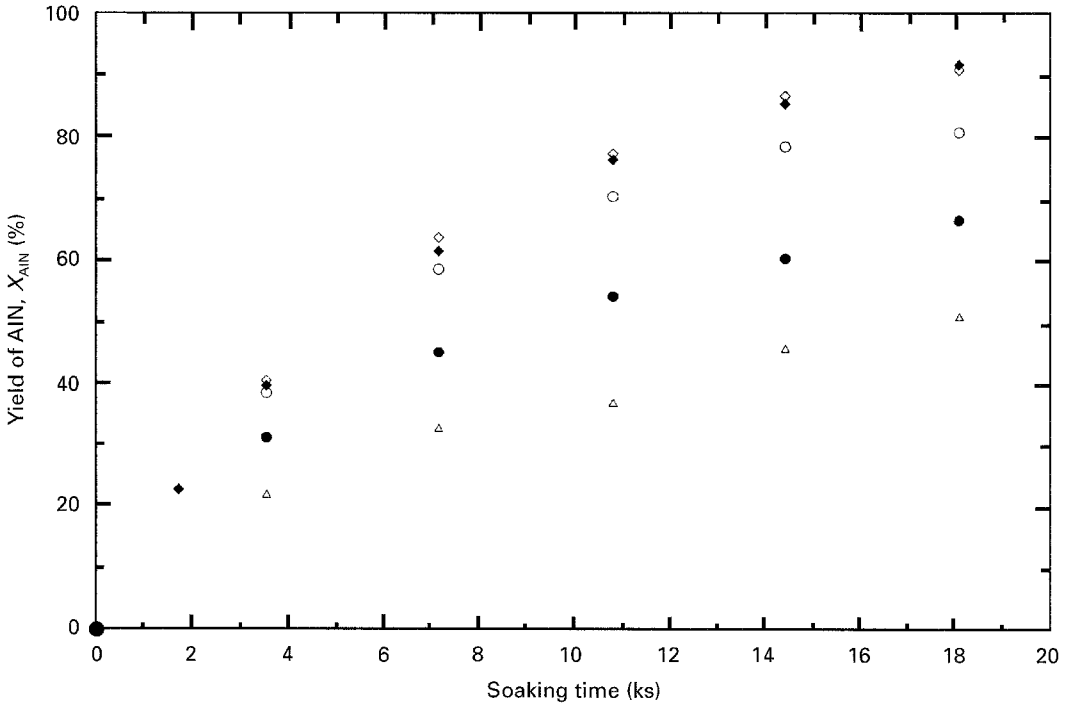

Figure 9 Plot of the yield of AlN against soaking time, showing the effect of sample height (m): (◇) 0.001, (◆) 0.002, (○) 0.004, (●) 0.006, (△) 0.008.

intrinsic. Therefore, sample heights in all experimental runs were maintained at 0.002 m.

3.2.3. Effect of reaction temperature

The experimental results shown in Fig. 10 indicate that the higher the reaction temperature, the faster will be the reaction. This result coincides with those of most previous investigators [4, 15].

3.2.4. Effect of molar ratio of $C/Al(OH)_3$

The effect of the molar ratio of $C/Al(OH)_3$ on the yield of AlN is depicted in Fig. 11. This figure reveals that

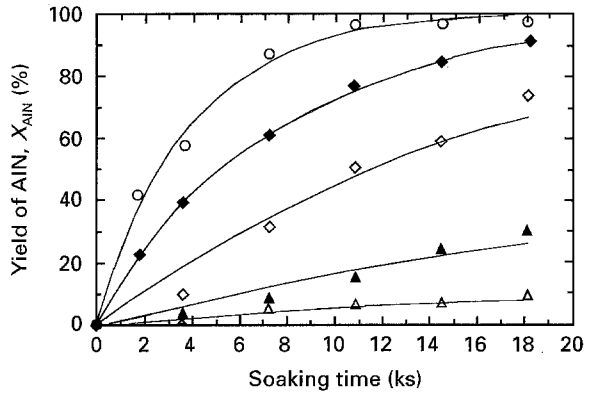

Figure 10 Plot of the yield of AlN against soaking time, showing the effect of reaction temperature (k): (△) 1573, (▲) 1623, (◇) 1673, (◆) 1723, (○) 1773.

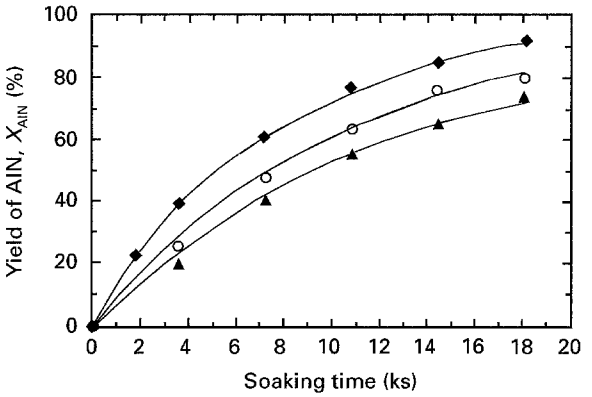

Figure 12 Plot of the yield of AlN against soaking time, showing the effect of carbon grain diameter (mm): (◆) 0.0420, (○) 0.0675, (▲) 0.1155.

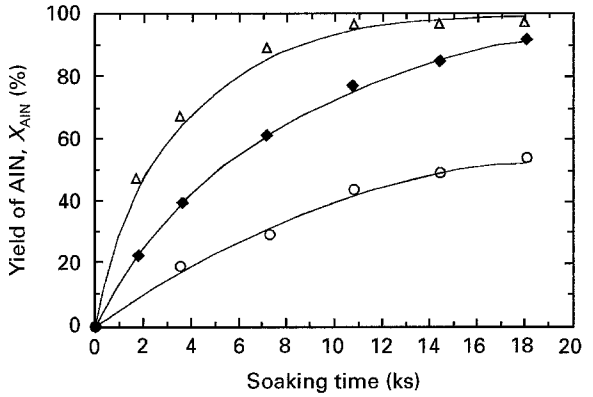

Figure 11 Plot of the yield of AlN against soaking time, showing the effect of molar ratio of $C/Al(OH)_3$: (△) 1.5/1, (◆) 3/1, (○) 6/1.

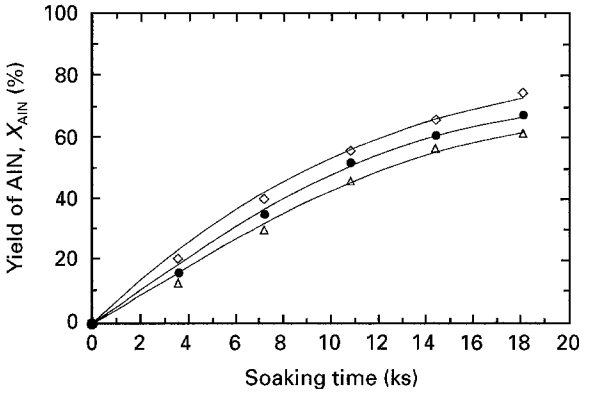

Figure 13 Plot of the yield of AlN against soaking time, showing the effect of $Al(OH)_3$ grain diameter (mm): (◇) 0.0420, (●) 0.0675, (△) 0.1155.

the higher the molar ratio of $C/Al(OH)_3$, the faster will be the reaction. Most investigators have obtained the same trend [3, 5, 15].

3.2.5. Effects of grain size

Two categories of experiments were performed in this series of reactions. In one category, the grain size of $Al(OH)_3$ was fixed and that of carbon was varied; in the other one, the grain size of carbon was fixed and that of $Al(OH)_3$ was varied. The results shown in Figs 12 and 13 indicate that the smaller the grain size of either $Al(OH)_3$ or carbon, the faster is the reaction. Many investigators have obtained the same results [6, 7, 9, 12].

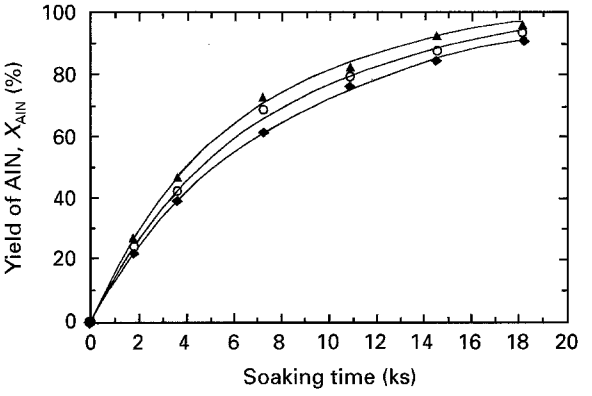

Figure 14 Plot of the yield of AlN against soaking time, showing the effect of initial bulk density (kg m^{-3}): (▲) 270, (○) 370, (◆) 510.

3.2.6. Effect of initial bulk density

Results obtained from this series of experiments are depicted in Fig. 14, revealing that when the initial bulk density was increased, the rate of reaction was decreased, but the effect was insignificant. The results agree with those of Mitomo and Yoshioka [10].

3.2.7. Reaction rate expressions

When the gas flow rate is sustained over 2.083×10^{-5} m^3 s^{-1} and the sample height is lower than 0.002 m, the overall reaction is rather close to chemical reaction control. The data obtained above are in this region. Hence, one can regress these data to obtain the intrinsic rate expression for the conversions

of $Al(OH)_3$ and carbon and the yield of AlN as follows

$$\frac{dC_{AlN}}{dt} = 1.104 \times 10^9 \exp[-322417(\text{J mol}^{-1})/RT]\, d_{Al(OH)_3}^{-0.285} d_C^{-0.573} \rho_0^{-1.611} C_{AlN}^{0.359} C_{Al(OH)_3}^{0.791} C_C^{0.868} \text{ mol s}^{-1} \quad (7)$$

$$-\frac{dC_{Al(OH)_3}}{dt} = 9.948 \times 10^8 \exp[-328819(\text{J mol}^{-1})/RT]\, d_{Al(OH)_3}^{-0.308} d_C^{-0.535} \rho_0^{-1.609} C_{AlN}^{0.335} C_{Al(OH)_3}^{0.799} C_C^{0.886} \text{ mol s}^{-1} \quad (8)$$

$$-\frac{dC_C}{dt} = 1.529 \times 10^{10} \exp[-349926(\text{J mol}^{-1})/RT]\, d_{Al(OH)_3}^{-0.603} d_C^{-0.508} \rho_0^{-2.067} C_{AlN}^{0.139} C_{Al(OH)_3}^{0.352} C_C^{1.682} \text{ mol s}^{-1} \quad (9)$$

where $C_{Al(OH)_3}$ is the number of moles of $Al(OH)_3$ at time t, C_C the moles of carbon at time t, $d_{Al(OH)_3}$ the grain diameter of $Al(OH)_3$ (m), d_C the grain diameter of carbon (m), R the gas constant = 8.314 kJ kg − $mol^{-1}K^{-1}$, T the reaction temperature (K), and ρ_0 the initial bulk density of the solid sample ($kg\,m^{-3}$). The applicable ranges for these rate expressions are: gas flow rate is higher than $2.083 \times 10^{-5}\,m^3\,s^{-1}$; sample height is less than 0.2×10^{-2} m; temperature range is between 1573 and 1773 K; molar ratio of $C/Al(OH)_3$ ranges between 1.5/1 and 6/1; grain diameter of carbon ranges between 0.42×10^{-5} and 0.1155×10^{-4} m; grain diameter of aluminium hydroxide ranges between 0.42×10^{-5} and 0.1155×10^{-4} m; the initial bulk density ranges between 270 and 510 $kg\,m^{-3}$.

In Equations 7–9, the higher the temperature, the higher the reaction rate is represented by the exponential terms; the smaller the grain sizes of $Al(OH)_3$ or carbon, the faster the reaction, is represented by the minus exponents of $d_{Al(OH)_3}$ and d_C in the rate expressions. When the value of the initial bulk density is changed, all the values of ρ_0, $N^0_{Al(OH)_3}$ and N^0_C are changed. Therefore, the effect of the initial bulk density cannot be represented alone by the exponents of ρ_0.

According to Equations 7–9, the relationships between conversions of $Al(OH)_3$ and carbon and the yield of AlN with reaction time can be calculated. They are shown by the solid lines in Figs 10–14. These figures reveal that the calculations correlate sufficiently with the measurements. Calculated curves have not been drawn for Figs 6–9, because resistance due to gas film mass transfer and intergrain gas diffusion cannot be ignored in these cases.

4. Conclusions

1. Aluminium hydroxide was dehydrated to aluminium oxide in a short period before it is reduced and nitrided to aluminium nitride.

2. AlON and Al_2O are intermediate products in this reaction system.

3. The reaction rate was found to be increased by increasing the nitrogen flow rate, molar ratio of $C/Al(OH)_3$ or reaction temperature.

4. The reaction rate was also found to be increased by decreasing the sample size, the grain sizes of carbon or aluminium hydroxide or the initial bulk density of the solid sample.

5. The rate expressions of conversions of $Al(OH)_3$ and carbon, as well as yield of AlN were determined on the basis of experimental data.

Acknowledgement

The authors thank the National Science Council, Taiwan, for financial support (Grant NSC 84-2214-E-011-001).

References

1. T. SAKAI and M. IWATA, *Yogyo-Kyokai-Shi* **82** (3) (1974) 181.
2. A. G. VODOPSANOV, A. V. SEREBRYAKOVA and G. N. KOZHEVNIKOV, *Izv. Akad. Nauk. SSSR. Met.* **1** (1982) 43.
3. H. L. WANG, MS thesis, Department of Mineral Metallurgy and Materials Science, National Cheng Kung University, Tainan, Taiwan (1988).
4. S. HIRAI, T. MIWA, T. IWATA, M. OZAWA and H. G. KATAYAMA, *J. Jpn Inst. Metals* **53** (1989) 1035.
5. A. TSUGE, H. INOUE, M. KASORI and K. SHINOZAKI, *J. Mater. Sci.* **25** (1990) 2359.
6. H. K. CHEN, C. I. LIN and C. LEE, *J. Am. Ceram. Soc.* **77** (1994) 1753.
7. Y. W. CHO and J. A. CHARLES, *Mater. Sci. Technol.* **7** (1991) 495.
8. M. ISH-SHALOM, *J. Mater. Technol.* **1** (1982) 147.
9. H. INOUE, A. TSUGE and K. KOMEYA, US Pat. 4680278 (1987).
10. M. MITOMO and Y. YOSHIOKA, *Adv. Ceram. Mater.* **2** (3A) (1987) 253.
11. *Idem*, US Pat. 4643859 (1987).
12. J. A. CHARLES and Y. W. CHO, UK Pat. Appl. GB 2233969A (1991).
13. L. CANDELA and D. D. PERLMUTTER, *AIChE J.* **32** (1986) 1532.
14. T. SATO, *Thermochim Acta* **88** (1) (1985) 69.
15. N. KURAMOTO and H. TANIGUCHI, US Pat. 4618592 (1986).

Received 12 October 1994
and accepted 15 December 1995